Journal of Hydrology 617 (2023) 129143

Contents lists available at ScienceDirect

Journal of Hydrology

journal homepage: www.elsevier.com/locate/jhydrol

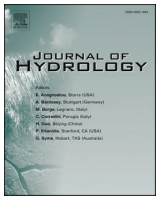

Research papers

Amplified future risk of compound droughts and hot events from a hydrological perspective

Sifang Feng, Zengchao Hao *, Yitong Zhang, Xuan Zhang, Fanghua Hao

College of Water Sciences, Beijing Normal University, Beijing 100875, China

ARTICLE INFO

Keywords:
Drought
Dry and hot
Compound events
CMIP6

ABSTRACT

Global warming can result in changes in droughts and hot events (or compound droughts and hot events, CDHEs), which can take a heavy toll on the society and environment. Recent studies have made substantial progress in the projection of these events. However, previous projection studies mostly focus on the concurrences of meteorological droughts and hot events but ignore the difference among various CDHEs. Specifically, the concurrence of hot events and different types of droughts (e.g., agricultural droughts and hydrological droughts) has been seldom explored from a hydrological perspective. Based on phase six of the Coupled Model Intercomparison Project (CMIP6), we evaluate changes in different types of CDHEs, including compound meteorological drought-hot events (CMDHEs), compound agricultural drought-hot events (CADHEs) and compound hydrological drought-hot events (CHDHEs), for different future periods at the global scale. Based on comparisons with data from Global Land Data Assimilation System Version 2 (GLDAS-2.0), CMIP6 can reproduce the overall spatial distribution and temporal variation of different CDHEs at the global scale. In addition, the frequency and spatial extent of the three compound events show a marked increase during different future periods relative to the base period 1995–2014. The projected increase in global average frequency of CMDHEs in the long term period is lower than that of CADHEs (increase by 73.74% and 113.95% for CMDHEs and CADHEs, respectively). The uncertainty in the simulation of CADHEs and CHDHEs is relatively larger than CMDHEs in the future periods over most regions. The results of this study highlight the urgent demand for adaptation measures of CDHEs to cope with compound extremes in the future.

1. Introduction

The concurrent or consecutive occurrences of multiple hazards or events are commonly termed compound events, which can lead to disastrous repercussions even though the individual hazards or/and events may not be extreme (Hao et al., 2022; Leonard et al., 2014; Zscheischler and Seneviratne, 2017). Among multiple types of compound events, compound droughts and hot events (CDHEs) at different time scales have attracted increasing attention recently (Feng et al., 2021; Li et al., 2022; Mukherjee et al., 2020; Sippel et al., 2018; Wang et al., 2016; Yuan et al., 2018; Zscheischler and Seneviratne, 2017). Multiple lines of evidence have shown that CDHEs may lead to a broader and larger impact on natural and social environments than do individual droughts or high-temperature extremes (Poschlod et al., 2020; Zhou et al., 2019; Zscheischler et al., 2020). For instance, significant impacts of CDHEs on food security, water resources, vegetation, settlements, and infrastructure over various regions have been observed in the past decades (Hao et al., 2022), such as 2003/2018 in Europe (Bastos et al., 2020; Fink et al., 2004) and 2010 in Russia (Trenberth and Fasullo, 2012). In addition, a consensus already exists that CDHEs have increased significantly in large regions of global land areas over the last few decades (Feng et al., 2021; Hao et al., 2013; Kirono et al., 2017; Manning et al., 2019; Mazdiyasni and AghaKouchak, 2015; Wu et al., 2021a; Zscheischler and Seneviratne, 2017). The significant impacts and increased occurrences of CDHEs call for an improved understanding of future changes in CDHEs, which can provide valuable information to risk managers, decision-makers, and engineers under a warming climate.

Recently, increased attention has been paid to the variation in high temperature accompanied by precipitation deficits (i.e., compound meteorological droughts and hot events, hereafter CMDHEs) during future periods based on climate model simulations from Phase 5 of Coupled Model Intercomparison Project (i.e., CMIP5) at the global scale (Mukherjee et al., 2022; Sarhadi et al., 2018; Weber et al., 2020; Wu

* Corresponding author at: No. 19, XinJieKouWai St., Haidian District, Beijing 100875, China.
E-mail address: haozc@bnu.edu.cn (Z. Hao).

https://doi.org/10.1016/j.jhydrol.2023.129143
Received 25 October 2022; Received in revised form 9 January 2023; Accepted 16 January 2023
Available online 19 January 2023

et al., 2021b; Zhan et al., 2020; Zscheischler and Seneviratne, 2017). For instance, based on CMIP5 simulations under the Representative Concentration Pathway (RCP) 8.5 scenario, Wu et al. (2021b) showed global area affected by CMDHEs will increase to about 1.7–1.8 times by the end of the 21st century relative to that during 1950–1999. As a new generation of climate models, CMIP6 simulations under different Shared Socioeconomic Pathway-Representative Concentration Pathway (SSP-RCP) scenarios combine both socioeconomic and technological development and fill gaps in previous RCPs in CMIP5 model simulations (O'Neill et al., 2016). The performance of CMIP6 models in CMDHEs (Ridder et al., 2021; Wu et al., 2021c) has been assessed to understand uncertainties in model simulations (Chen and Yuan, 2022; Muthuvel et al., 2023). For instance, the useful skills of the CMIP6 models in capturing the simultaneous occurrence of heat waves and meteorological drought has been found in large regions including North America, Europe, and Eurasia (Ridder et al., 2021). Based on CMIP6 simulations, extensive studies have highlighted the potential increase in CMDHEs in the future periods with continued global warming (Meng et al., 2022; Ridder et al., 2022; Vogel et al., 2020; Wu et al., 2021c; Zhang et al., 2022).

Arguably, a meteorological drought over an extended period due to precipitation deficits may further result in depleted soil moisture (i.e., agricultural droughts) and declined runoff/streamflow (i.e., hydrological droughts) (Van Loon, 2015; Vicente-Serrano et al., 2022). Different types of droughts have increased in large regions along with enhanced temperature-related extremes for historical periods (Dai, 2013; Spinoni et al., 2014; Vicente-Serrano et al., 2022), which may increase the likelihood of concurrence of temperature extremes and agricultural (hydrological) droughts, plaguing agricultural systems (or crippling energy sectors). Recent studies have paid increasing attention to the changing patterns of agricultural (hydrological) droughts accompanied by high temperatures. For instance, high-temperature extremes or enhanced atmospheric evaporative demand (AED) can increase evapotranspiration, dry out vegetation and soil (Luo et al., 2017; Miralles et al., 2019) and further cause depleted water resources (e.g., runoff, streamflow, lake, and groundwater) (Brunner et al., 2021; Das et al., 2011; Vicente-Serrano et al., 2014; Woodhouse et al., 2016), which may damage agricultural production, affect the domestic water supply, and reduce hydropower generation (Feng et al., 2022). Under anthropogenic global warming, temperature will continue to rise in the future, which may further increase the concurrence of high temperatures and different types of droughts in the coming decades. The potential increase of these extremes can result in risks that may cascade across sectors and regions (IPCC, 2022), highlighting the paramount importance of risk assessments of CDHEs based on different drought types (or different stages of the water cycle) in the future. However, projections of different types of CDHEs for future periods on a global scale are still lacking.

The objective of this study, therefore, is to assess the spatial and temporal variation in different compound droughts and hot events for the future period on a global scale. Based on climate model simulations from CMIP6, we first evaluate changes in different types of CDHEs during the historical period through comparisons with the reference data from Global Land Data Assimilation System (GLDAS). We then project the changes in CDHEs for different future periods. We focus on the SSP5-8.5 scenario, which assumes "the worst scenario" pathway (O'Neill et al., 2016; Wang et al., 2021). Building on these assessments, we try to answer two questions: (1) How do CMIP6 models perform in simulating different types of compound events? (2) What is the difference in variation of different types of compound events during future periods under the SSP5-8.5 scenario?

2. Data and Methods

2.1. Data

2.1.1. GLDAS

To assess the performance of CMIP6 models, we obtain monthly temperature, total precipitation, soil moisture, and surface runoff from the Global Land Data Assimilation System Version 2 (GLDAS-2.0). The GLDAS-2.0 data with a 0.25-degree resolution spanning 1948–2014 are provided by the National Aeronautics and Space Administration (NASA) (Rodell et al., 2004). The soil moisture from GLDAS is divided into four vertical layers including 0–10 cm, 10–40 cm, 40–100 cm, and 100–200 cm. Here, we focus on the shallow 0–10 cm soil moisture. All variables are re-gridded to the same resolution of $2^\circ \times 2^\circ$ with CMIP6 models based on the nearest-neighbor interpolation.

2.1.2. CMIP6 multi-model ensemble

Simulations of monthly 2-m near-surface air temperature (tas), total precipitation rate (pr), top 10 cm soil moisture content (mrsos), and total surface runoff (mrros) from CMIP6 models are selected for this study, which includes simulations for the historical period (1955–2014 in this study) and future periods. Following Intergovernmental Panel on Climate Change (IPCC) Sixth Assessment Report (AR6) (IPCC, 2022), we select three periods (i.e., 2021–2040, 2041–2060, and 2081–2100) to define near term, mid-term, and long term to assess the future risk of compound events. Models that include variables of interest for two experiments (historical and SSP5-8.5) are selected. In total, we selected thirteen models (Table S1) for the model evaluation and future projection. All CMIP6 model outputs are re-gridded to the common resolution ($2^\circ \times 2^\circ$) based on the nearest-neighbor interpolation. In this study, the multi-model ensembles (MMEs) are constructed by using equal weights to all thirteen models (i.e., the multi-model ensemble means, hereafter MMEM) to reduce uncertainties resulting from model differences.

2.2. Methods

2.2.1. Identification of compound events

There are different ways to define CDHEs, such as the combined threshold approach (Feng et al., 2021; Ridder et al., 2022; Zscheischler et al., 2018) and joint distribution approach (Muthuvel and Amai, 2022; Muthuvel et al., 2023; Shah and Mishra, 2020). Here we apply the combined threshold approach to define CDHEs on a monthly time scale. This non-parametric approach is easy to implement without making assumptions about the distribution family. The hot conditions and droughts are identified using multiple variables, namely temperature (T) for hot conditions, precipitation (P) for meteorological drought, shallow soil moisture (S) for agricultural drought, and surface runoff (R) for hydrological drought. At each grid point, a compound event is considered to occur when the temperature is higher than a relative threshold and precipitation (soil moisture, surface runoff) is lower than a threshold at the same time. Specifically, compound droughts and hot events are defined based on the concurrence of drought variables (i.e., precipitation, soil moisture, and runoff) below the 50th percentile and temperature above the 50th percentile for each month during the period of interest (i.e., historical periods and three future periods). The thresholds of each variable are defined based on the base period (1995–2014), which is adopted by IPCC (IPCC, 2021). In addition, plenty of major extreme events have occurred in this timeframe including the Millennium droughts (1997 to 2010) in Australia (Yildirim et al., 2022), extreme droughts in China from 2000 to 2002 (Zhang et al., 2019), and the severe droughts in south Asia during 2002 (Muthuvel and Amai, 2022). Thus, applying the thresholds from this period can help us compare future extremes with these major extreme events in recent decades. Building on this, three types of compound events can be defined for further analysis, including compound meteorological droughts and hot events (CMDHEs, T50/P50), compound agricultural

droughts and hot events (CADHEs, T50/S50), and compound hydrological droughts and hot events (CHDHEs, T50/R50).

2.2.2. Characteristics of compound events

We mainly focus on the frequency and spatial extent of CDHEs to assess the spatial and temporal variation. Here, the frequency of compound events (f_{DH}) for each grid during a specific period is defined as the number of months with occurrences of CDHEs (N_1) divided by the total number of months (N) and then multiplied by 100 (unit: %), which can be expressed as:

$$f_{DH} = \frac{N_1}{N} * 100\% \tag{1}$$

In addition, the annual spatial extent (s_{DH}) is defined as the number of grids covered by compound events (averaged occurrence of 12 months for each year) divided by the total number of grid points over the global land area, which can be expressed as:

$$s_{DH} = \frac{\sum_{i=1}^{I}\sum_{m=1}^{12} O_{m,i}}{I \times 12} \times 100\% \tag{2}$$

where $O_{m,i}$ is the occurrence (i.e., 0 or 1) of CDHEs in month m at grid i; I is the total number of grid points over global land area.

Building on this, we first compare the spatial distribution of frequency (f_{DH}) and temporal variation of spatial extent (s_{DH}) based on GLDAS and CMIP6 models during the historical period 1955–2014 (historical simulation data from CMIP6 models extend to 2014). The relative change (RC) in the number of compound events during three future periods (i.e., 2021–2040, 2041–2060, and 2081–2100) compared with that during the base period 1995–2014 can be expressed as follows:

$$RC = \frac{N_f - N_b}{N_b} \times 100\% \tag{3}$$

where N_b and N_f are the number of compound events in the base period and future period, respectively.

2.2.3. The Mann-Kendall (MK) trend and Sen's slope test

To assess the trend of changes in the spatial extent of different compound event types, we apply the MK trend test (Kendall, 1975; Mann, 1945). Here, the Sen's slope is applied to detect the magnitude of the linear trend of spatial extent, which can be calculated:

$$\beta = Median\left(\frac{x_j - x_i}{j - i}\right) \tag{4}$$

where β represents the slope of the trend test; x_i and x_j represent sample values ($i < j$) for the time series x_t ($t = 1, 2, \ldots, n$); n indicates the length of spatial extent series.

3. Results

3.1. Model evaluation

3.1.1. Frequency distribution of CDHEs

To evaluate the performance of CMIP6 models, the spatial distributions of the frequency of three compound events (CMDHEs, CADHEs, and CHDHEs) are calculated first (See Methods). Fig. 1 illustrates the spatial distribution of the frequency of different types of compound events based on GLDAS and CMIP6 during the historical period from 1955 to 2014. The frequency of three compound events shows an overall consistent pattern, which is related to the propagation of meteorological drought to agricultural/hydrological drought (Afshar et al., 2022; Feng et al., 2023; Zeng et al., 2022; Zhu et al., 2021). Specifically, the regions with relatively low soil moisture and surface runoff generally correspond well to the dry center of precipitation and vice versa during the historical period (Qiao et al., 2022). A high frequency of CMDHEs, CADHEs, and CHDHEs in central North America, northern South America, eastern Europe, southern Asia, and eastern China is observed from GLDAS. These regions with a high frequency of compound events are generally consistent with results from CMIP6, as shown in Fig. 1(d-f), indicating that CMIP6 models can reproduce the overall spatial distribution of the three types of CDHEs.

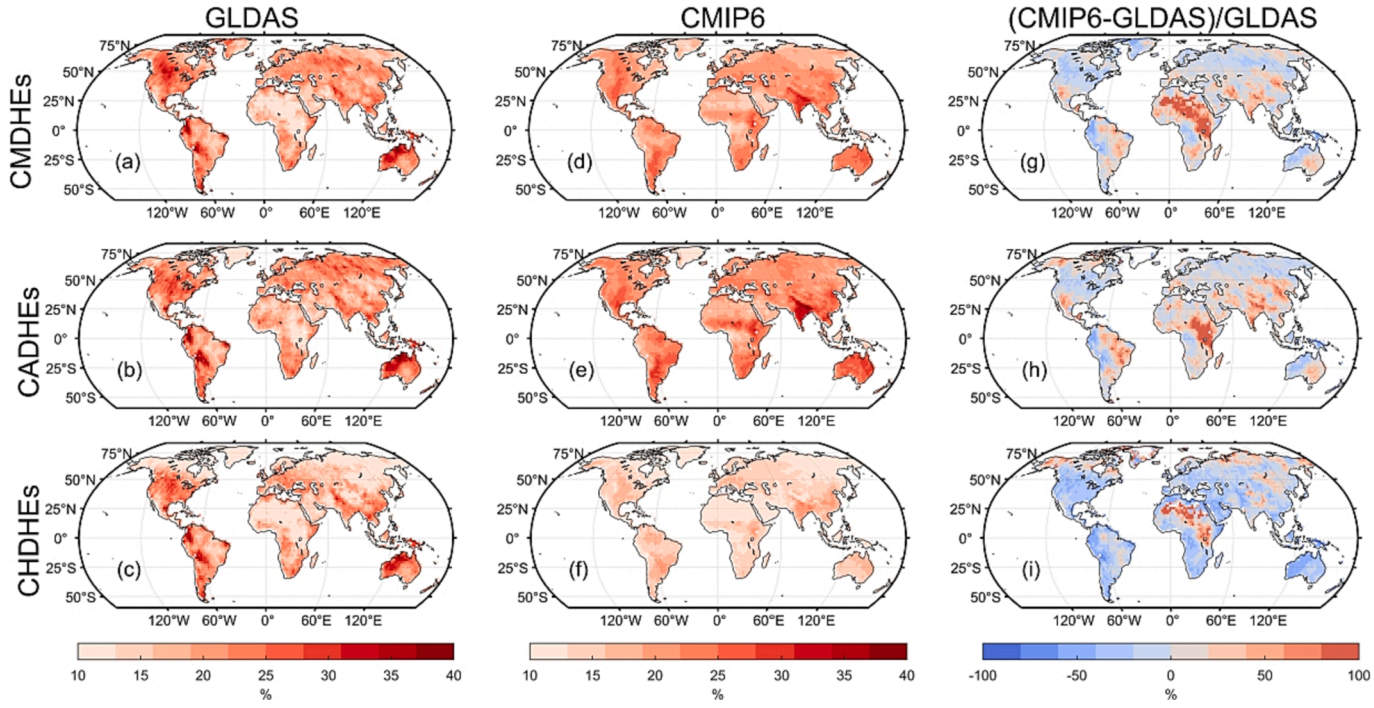

Fig. 1. Spatial distribution of the frequency of three compound events (i.e., CMDHEs, CADHEs, and CHDHEs) based on GLDAS and CMIP6 multi-model mean during the historical period from 1955 to 2014. (a)-(c) GLDAS; (d)-(f) CMIP6; (g)-(i) difference between GLDAS and CMIP6 measured by relative biases defined as (CMIP6-GLDAS)/GLDAS × 100 %.

To further analyze the frequency difference between GLDAS and CMIP6, the relative bias between GLDAS and CMIP6 is shown in Fig. 1 (g-i). These assessments reveal that a positive bias exists for CMDHEs in certain regions (49.99 % of total grids), such as eastern South America, most of Africa, southern Asia, and eastern Australia. The performance of CMIP6 models in simulating compound events is related to the simulation performance of individual variables. For example, previous studies have shown that simulated precipitation from CMIP6 is underestimated in South America and central Africa compared with GLDAS (Qiao et al., 2022), which may contribute to the higher frequency of CMDHEs in CMIP6 than that in GLDAS in these regions. For CADHEs, a comparison of the CMIP6 and GLDAS reveals a positive bias in large regions (57.30 % of total grids), such as eastern South America, most of Africa, southern Asia, and eastern Australia. This may be related to the lower surface soil moisture simulated by CMIP6 compared with GLDAS in these regions (Qiao et al., 2022), which likely induces more CADHEs in CMIP6 models. For CHDHEs, the bias between GLDAS and CMIP6 is largely negative in most regions (about 70.00 % of total grids), which is probably because those CMIP6 models produce high levels of surface runoff compared with that from GLDAS (Qiao et al., 2022), causing a small number of CHDHEs in CMIP6.

A more detailed look at the regional difference in the frequency of CDHEs for six continents (i.e., North America, South America, Europe, Africa, Asia, and Australia) between GLDAS and CMIP6 during 1955–2014 is provided in Fig. 2 (with the relative bias between GLDAS and CMIP6 shown in Table 1). CMIP6 model can reproduce the comparative relationship of the three types of compound events in GLDAS (e.g., the frequency of CADHEs is the highest in almost all continents). High consistency between model simulations and GLDAS exists over Europe with a low relative bias for CMDHEs. Larger differences between the frequency of CADHEs and CHDHEs from GLDAS and CMIP6 simulations are shown in Africa and Australia.

3.1.2. Historical spatial extent of CDHEs

We then compare temporal changes in the annual spatial extent of the three types of compound events from 1955 to 2014 across the globe (Fig. 3). The temporal variation in the spatial extent from CMIP6 has relatively high Pearson correlation coefficients with GLDAS (i.e., 0.84, 0.85, and 0.85 for CMDHEs, CADHEs, and CHDHEs, respectively), which indicates a relatively good simulation performance from CMIP6 models at the global scale. The temporal variation highlights a significant increase in the spatial extent of three compound events (CMDHEs, CADHEs, and CHDHEs) based on GLDAS, especially after the 1990s (Fig. 3), which is generally simulated well from CMIP6 models. For example, the slopes of the spatial extent of CMDHEs are 2.55 %/decade and 2.68 %/decade based on GLDAS and CMIP6, respectively. Meanwhile, the comparative relationship of spatial extent among three compound events is overall consistent in both datasets. Specifically, the slope of the spatial extent of CADHEs (2.80 %/decade) is the highest, followed by CMDHEs (2.68 %/decade) and CHDHEs (1.87 %/decade) based on CMIP6 models, which is highly consistent with the results in GLDAS (i.e., 2.80 %/decade, 2.55 %/decade, and 2.30 %/decade for CADHEs, CMDHEs, and CHDHEs, respectively). Moreover, we also find larger variability (shaded area) in the simulation of CHDHEs, as shown in Fig. 3(c).

At the continental scale, a consistent increase in the spatial extent of different types of CDHEs (with a high correlation between results from GLDAS and CMIP6) is also shown in almost all continents in Fig. S1. However, some exceptions exist in certain continents, such as Australia. Specifically, the correlation coefficient of the spatial extent of those compound events between CMIP6 models and GLDAS over Australia is relatively low (non-significant). It indicates the low performance of CMIP6 models in simulating CDHEs in Australia, which is consistent with previous studies (Ridder et al., 2021).

3.2. Projection of hydro-meteorological variables

Since changes in compound events are highly dependent on changes in individual variables, we first assess changes in global mean temperature, precipitation, soil moisture, and runoff in the 21st century under the SSP5-8.5 scenario. Fig. 4 shows simulations from thirteen CMIP6 models in this study. These simulations show a continuing increase in temperature from 2021–2040 to 2081–2100 (compared with the base period 1995–2014). Higher temperature tends to lead to greater rates of evapotranspiration, which may cause a higher frequency of agricultural drought, as shown by the significant decline of soil moisture in Fig. 4. For example, the soil moisture changes from −0.81 % to −4.12 % from 2021–2040 to 2081–2100 compared with that during the base period.

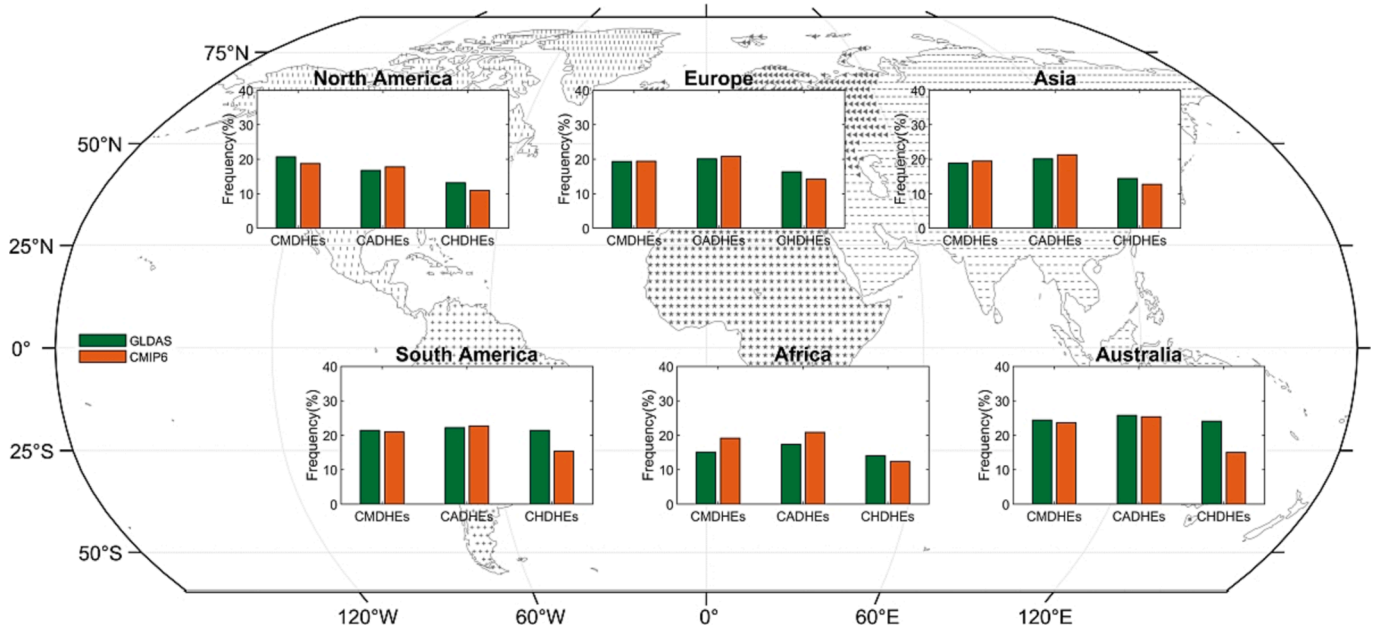

Fig. 2. Comparison of the frequency of three compound events (i.e., CMDHEs, CADHEs, and CHDHEs) over six continents (i.e., North America, South America, Europe, Africa, Asia and Australia) based on GLDAS and CMIP6 during the historical period (1955–2014).

Table 1
The relative bias of the frequency between GLDAS and CMIP6, defined as (CMIP6-GLDAS)/GLDAS × 100 %, over six continents from 1955 to 2014 based on Fig. 2.

	North America	South America	Europe	Africa	Asia	Australia
CMDHEs	−9.43 %	−2.27 %	0.34 %	26.30 %	3.19 %	−3.30 %
CADHEs	6.12 %	2.41 %	3.41 %	19.71 %	5.85 %	−1.47 %
CHDHEs	−16.40 %	−28.23 %	−13.41 %	−11.76 %	−11.55 %	−37.52 %

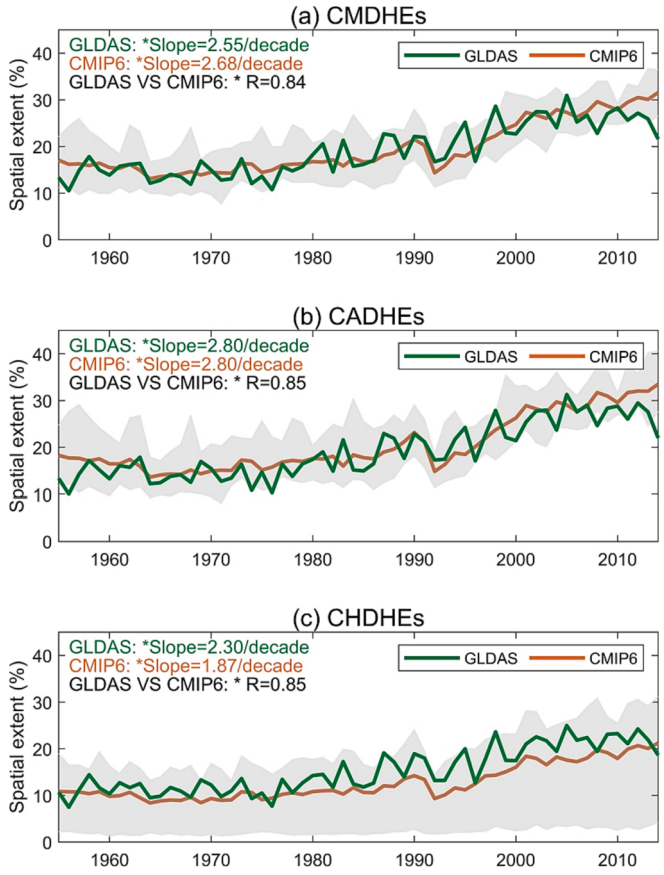

Fig. 3. Temporal changes in the spatial extent of CMDHEs (a), CADHEs (b), and CHDHEs (c) based on GLDAS and CMIP6 multi-model mean during the historical period 1955–2014. The slope of spatial extent is calculated by the Sen's slope estimator. R indicates the Pearson correlation coefficient of spatial extent between GLDAS and CMIP6. The asterisk (*) indicates the significant trend (and correlations) at a 0.05 significance level. The shaded area indicates the 5th-95th percentile ranges.

There is also an increase in mean precipitation (runoff), which changes from 1.66 % (0.10 %) in 2021–2040 to 8.27 % (0.13 %) in 2081–2100. Different directions of individual variables changes (also shown at different continents in Fig. S2) may cause complicated changes in corresponding compound events in the future. Thus, given the interwoven and nonlinear relationships among temperature and hydrometeorological elements (i.e., precipitation, soil moisture, and runoff) in the future, it is imperative to evaluate the compound events that span different aspects of the hydrologic cycle (i.e., CMDHEs, CAHDEs and CHDHEs) in a warmer climate.

3.3. Global projection of compound events

3.3.1. Change in frequency

To assess the future variation of three types of compound events, we show the relative changes (RC) in the frequency of CMDHEs, CADHEs, and CHDHEs during three future periods (i.e., near term, mid-term, and long term) under the SSP5-8.5 scenario. Overall, the frequency of three types of compound events (i.e., CMDHEs, CADHEs, and CHDHEs) is projected to increase in the three future periods compared with the base period 1995–2014 (Fig. 5). The increase in the frequency of different types of CDHEs is consistent over northern South America, parts of Europe, and the Mediterranean region, which is likely related to enhanced temperature and decreased precipitation (shallow soil moisture, and surface runoff) over these regions in a warming climate (Fig. S3) (Aadhar and Mishra, 2020; Cook et al., 2020; Dutta and Maity, 2022; Li and Li, 2022; Naumann et al., 2018; Stevenson et al., 2022; Ukkola et al. 2020; Vicente-Serrano et al., 2022; Zhao and Dai, 2022). In addition, a slight increase or even decrease in frequency for three compound events is projected in some regions, such as parts of extra-tropical South America, eastern Africa, and southern Asia. This is likely related to the increase in precipitation (soil moisture, surface runoff) over those regions, as shown in Fig. S3.

For CMDHEs, the average frequency of CMDHEs over global regions with the high model agreement (more than 80 % of the models agree on the sign of changing pattern) enhances by 43.87 % during the near term, which increases to 73.74 % in the long term compared with that during the base period. Compared with CMDHEs, the increase in CADHEs is larger and more widespread in most regions. Some evidence has indicated that agricultural drought based on soil moisture is more widespread than drought estimated using precipitation under SSP5-8.5 by the end of the twenty-first century (Cook et al., 2020), which further causes more CADHEs than CMDHEs. We confirm that this conclusion generally holds when employing more extreme thresholds than the 50th percentile (e.g., the results based on the 30th and 70th percentile are shown in Fig. S4). Note that some regions with only a marginal increase in CMDHEs (like northern North America and Eurasia) are projected to experience a remarkable increase in CADHEs. Precipitation is the most important and direct factor among others affecting soil moisture (Zhang et al., 2008) and the wetting of soil caused by precipitation is an intuitive process in nature (Koster et al., 2004; Koster et al., 2003). However, for some large regions like Eurasia covering an extensive range of longitudes and latitudes, the variables that can affect soil moisture are more complicated and diverse, which may cause a more complex land–atmosphere interaction and make the influence of precipitation on soil moisture weaker (Sang et al., 2021). This highlights that precipitation is not the only determinant of soil moisture and other significant processes (e.g., enhanced evaporative demand, increased plant water use) affecting soil moisture also change with warming (Cook et al., 2020; Hua et al., 2022; Yuan et al., 2021), which may cause more concurrence of agricultural drought and high temperature (i.e., CADHEs) in these regions under a warming climate.

An extensive and significant increase of CHDHEs is shown in large regions, like northern North America, Eurasia, southern Africa, and Australia, as shown in Fig. 5(g–i). Note that an increase in precipitation over certain regions may not directly translate to enhanced surface runoff. For example, precipitation is projected to increase over the middle to high latitudes of Northern Hemisphere due to increased specific humidity and increased water vapor transport from the tropics (Dutta and Maity, 2022; IPCC, 2021; Li and Li, 2022); however, surface runoff decreases in western North America, Canada, and western Russia (Cook et al., 2020), as shown in Fig. S3. In addition, we did not find a consistent pattern between changes in CADHEs and CHDHEs based on different thresholds (e.g., the relative change in CADHEs is similar to that in CHDHEs in Fig. 5, while the relative change in CHDHEs is larger than CADHEs based on a higher threshold, as shown in Fig. S4), which

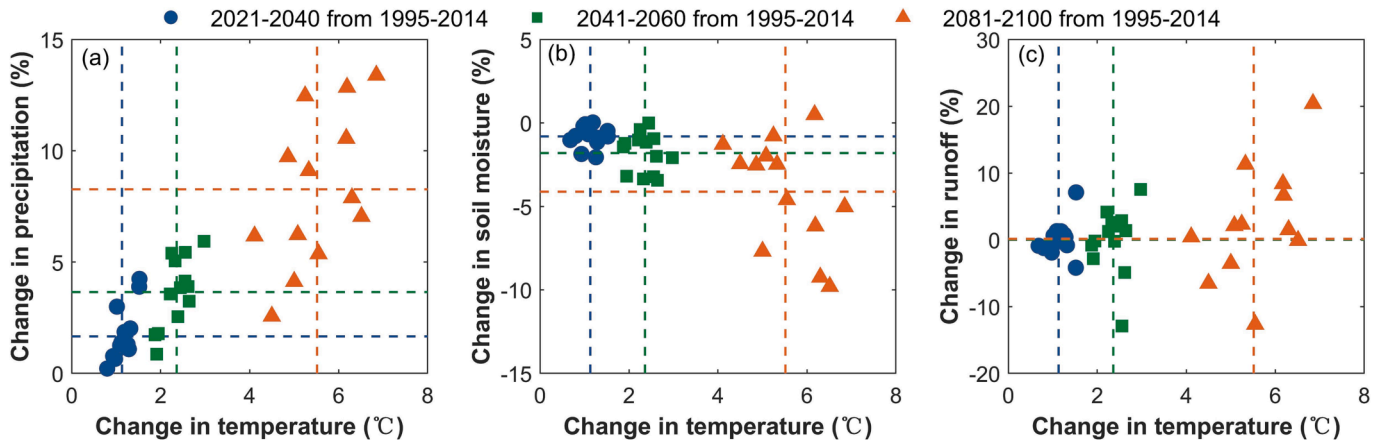

Fig. 4. Changes in mean global land surface precipitation (a), shallow soil moisture (b), and surface runoff (c) versus temperature for the near term (2021–2040), mid-term (2041–2060), and long term (2081–2100) relative to the baseline period (1995–2014) for each CMIP6 model. The dashed lines indicate the multi-model ensemble means of individual variables in different future periods. The markers with the same color and shape indicate thirteen CMIP6 models during specific future periods.

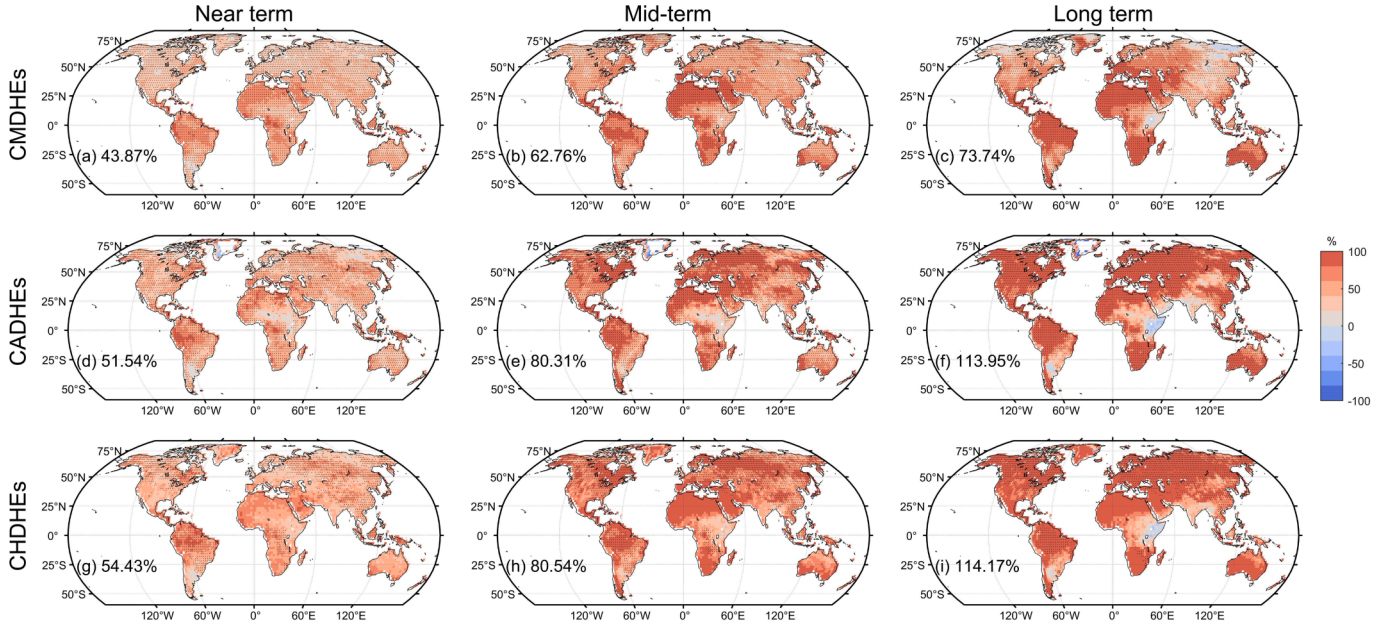

Fig. 5. The relative change in the frequency of different types of compound events for the near term (2021–2040), mid-term (2041–2060), and long term (2081–2100) relative to the baseline period (1995–2014) based on multi-model ensemble mean of CMIP6 models. Black stippling indicates that more than 80% of the models agree on the sign of changing pattern (negative or positive). The text in the left-bottom of each sub-figure indicates the mean of relative change in the frequency over regions with black stippling.

may be related to complex influencing factors of runoff (e.g., watershed features, snow, and vegetation) or uncertainties associated with limited samples from extreme thresholds.

3.3.2. *Change in spatial extent*

We further assess temporal changes in the spatial extent of different types of compound events from 2015 to 2100 and calculate changes in the slope of spatial extents, as shown in Fig. 6. The significant increase in the spatial extents of CMDHEs, CADHEs, and CHDHEs is projected for different future periods. The average spatial extent of three CDHEs generally increases from near term to long term period, as shown in Fig. 6(b). This indicates that more areas will be affected by CDHEs in the future under the SSP5-8.5 scenarios. The increased spatial extent of CMDHEs is accompanied by increased coverage of high temperatures and decreased coverage of meteorological droughts (based on precipitation), as shown in previous studies (Zeng et al., 2022) and Fig. S5, indicating the dominant role of temperature in driving the variation of CMDHEs. CADHEs have the largest increase in spatial extent, which is likely due to the increased coverage of both agricultural drought and high temperature (Fig. S5). The spatial extent of hydrological droughts shows a slight increase (not significant) (Fig. S5), which contributes to less increase in the spatial extent of CHDHEs compared with that of CADHEs (Fig. 6).

For the three future periods, the slope of changes in different types of CDHEs decreases from the near term to the long term period, as shown in Fig. 6(c). For instance, the slope of spatial extent for CMDHEs changes from 3.28 %/decade to 1.90 %/decade from the near term to the mid-term and even shows a slight downward trend during the long term (-0.55 %/decade). The slope of the increased spatial extent of high temperature decreases from the near term to long term period (from 8.25 %/decade to 0.57 %/decade) as shown in Fig. S5, which is consistent with the pattern of slope variation in different types of

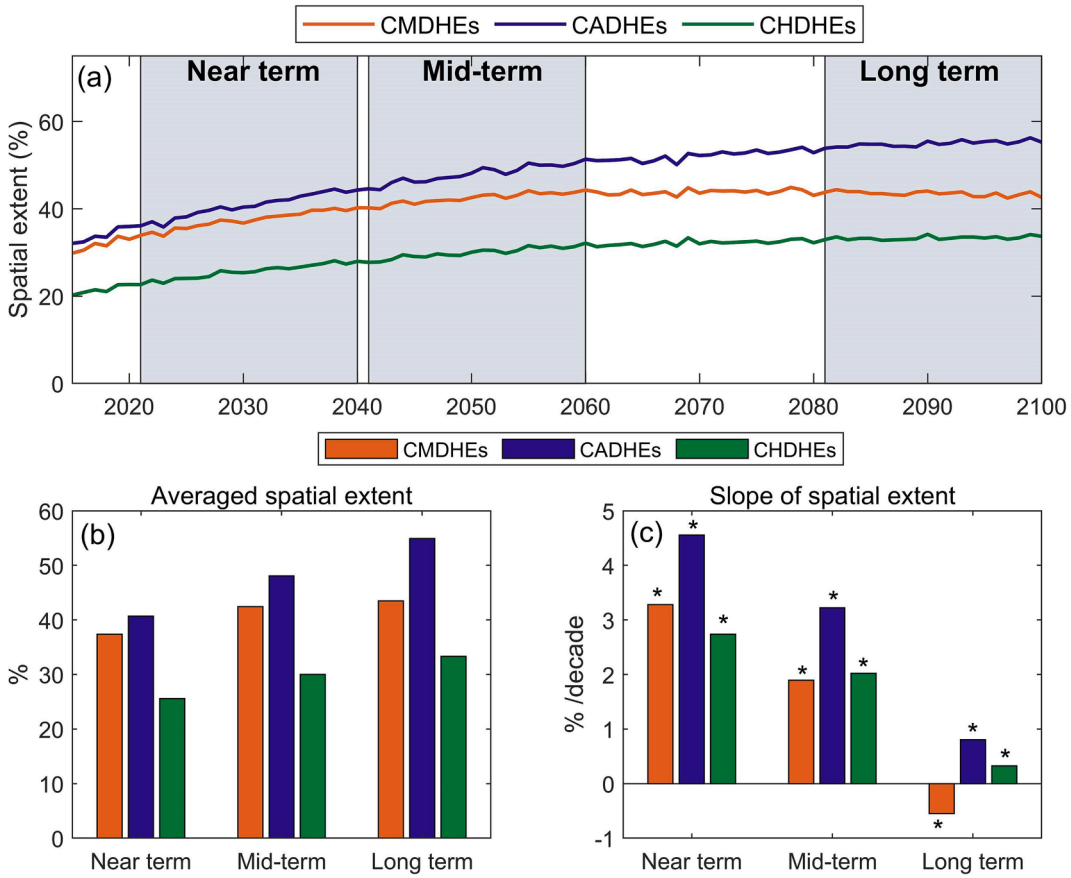

Fig. 6. (a) The spatial extent of three compound events (i.e., CMDHEs, CADHEs, and CHDHEs) from 2015 to 2100. The rectangular shadows represent the three future periods (i.e., near term, mid-term, and long term). (b) The average spatial extent during different future periods. (c) The slope of spatial extent (unit: %/decade) with the asterisk (*) indicating significant trends at a 0.05 significance level.

CDHEs. The slope (and changes) in the spatial extent of three types of droughts during the three periods are diverse (Fig. S5), such as the decreasing spatial extent of meteorological drought and increasing spatial extent of agricultural drought (Zeng et al., 2022; Zhao and Dai, 2022). The slope of the spatial extent of agricultural drought decrease from the near term to the long term period (with the slope of 1.32 %/decade, 1.22 %/decade, and 0.61 %/decade for the near term, mid-term, and long term, respectively). An increase but non-significant pattern from near term to long term applies to the changes in hydrological drought. Overall, the three compound events will continue to increase by the end of the 21st century, but the increase rate will gradually decrease in the future (associated with diverse changes in the spatial extent of individual variables).

3.3.3. Regional projection and uncertainty

Following IPCC AR6 WGI reference regions (Iturbide et al., 2020), the global land can be divided into 44 regions (Fig. S6). Based on that, we then assess the regional change in the frequency (unit: %, see Methods) of different types of compound events during three future periods, relative to the base period (1995–2014) over these regions (Fig. 7). The frequency of different types of compound events in the future will increase over most regions and a larger increase is projected during the long term period. The high increases are shown in several regions, such as S.Central-America (SCA) for CMDHEs, the Mediterranean (MED) for CADHEs and CHDHEs in the long term.

We also assess the uncertainty in the simulation of CDHEs at the regional scale by defining the uncertainty as the difference between the 75th and 25th quantiles of the box (Greve et al., 2018; Wu et al., 2021c). The uncertainties among the models are relatively small for CMDHEs relative to CADHEs and CHDHEs as shown in Fig. 7. For most regions, the uncertainties during the long term are larger than that during other future periods. Specifically, the percentages of regions with maximum variability (between 25th and 75th quantiles) in the long term compared with other future periods for the three compound events are 70.45 % (CMDHEs), 81.82 % (CADHEs), and 81.82 % (CHDHEs), respectively. Such uncertainty can result from multiple factors (e.g., physical parameterization and internal variability) and needs further investigation in the future.

4. Discussion

4.1. Implication

The development of different drought types in the hydrological cycle (i.e., drought propagation) has attracted increasing attention in recent decades (Gevaert et al., 2018; Van Lanen et al., 2013; Wu et al., 2018). Under anthropogenic global warming, the persistence of warm temperatures and drought propagation highlights the temporal linkage among different types of compound events in the hydrological cycle (Feng et al., 2023), which may take a toll on the socioeconomics and ecosystems. In this study, we find a significant increase in frequency for CMDHEs, CADHEs, and CHDHEs in different future periods. A higher increase in the frequency of three types of CDHEs is projected in large regions (e.g., northern South America, and Europe), which underlines the amplified risk of increased CDHEs in a warmer climate. The CADHEs and CHDHEs based on soil moisture and surface runoff, respectively, show different spatial responses (e.g., sign and magnitude of variations) to CMDHEs in some regions. Thus, these compound events cannot

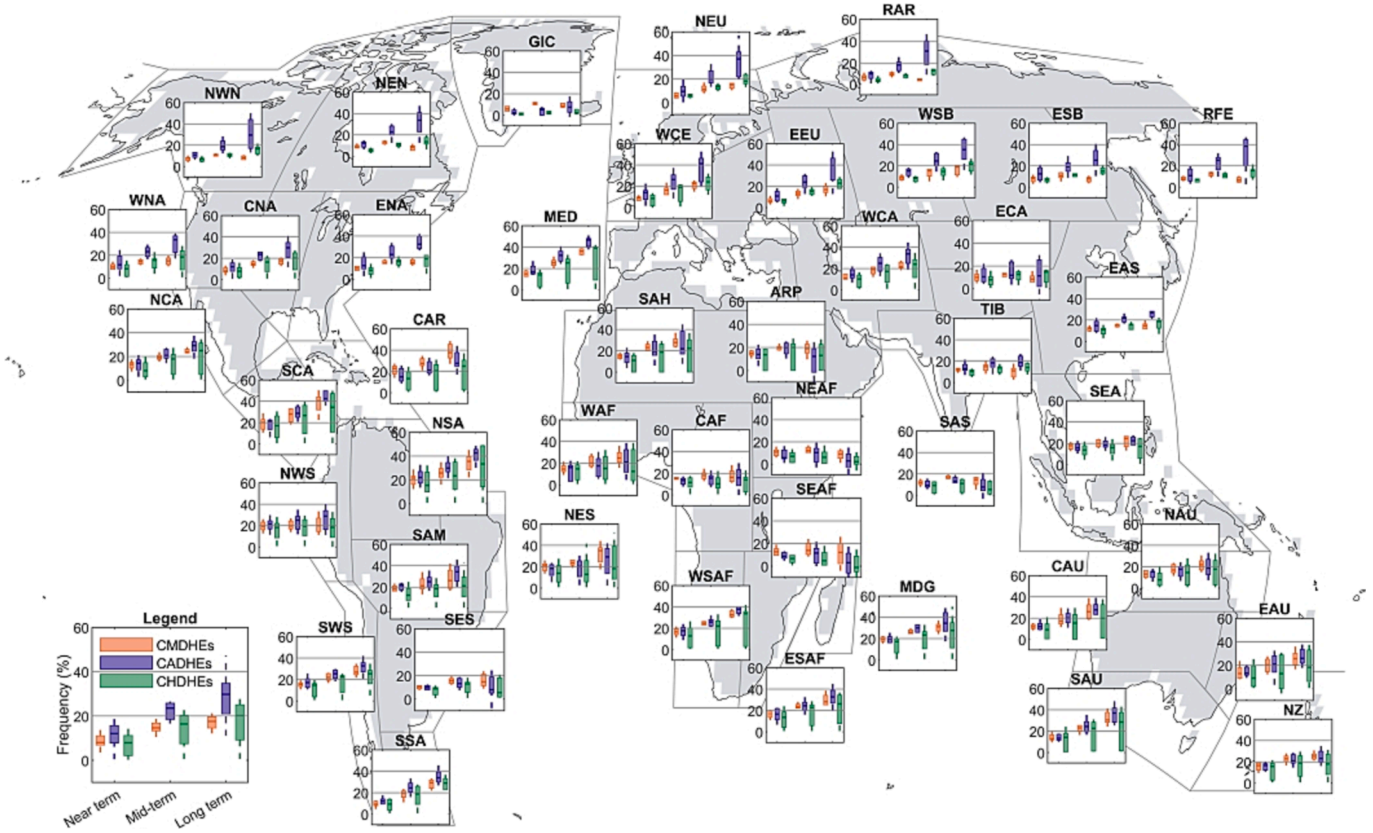

Fig. 7. The absolute changes in the frequency of three compound events (CMDHEs, CADHEs, and CHDHEs) over 44 regions for the near term (2021–2040), mid-term (2041–2060), and long term (2081–2100) relative to the baseline period (1995–2014) under the SSP5-8.5 scenario. The box plots show uncertainties among the thirteen CMIP6 models.

substitute as alternatives for each other, highlighting the importance and necessity of considering the response of different types of compound events to climate change from the hydrologic cycle perspective.

4.2. Limitation

There are some limitations in this study regarding the inherent uncertainty from climate model simulations and indicator/threshold selection. Although there is robust agreement on the sign of the variations in the frequency of three types of compound events in large regions (Fig. 5), large discrepancies in the magnitude (or even sign) of these changes among the CMIP6 models exist (as shown in Fig. 7). Due to the inherent uncertainties in the simulations of precipitation (soil moisture, runoff) and temperature in CMIP6 models (Hou, et al., 2023; Ukkola et al., 2020; Zhao and Dai, 2022), uncertainty analysis and quantification in the projection of multiple types of CDHEs should be conducted in future studies based on different CMIP6 models. In addition, previous studies highlighted a different changing pattern of surface and total soil moisture drought in some regions like America and Europe (Zhao and Dai, 2022). Besides, this study only focuses on surface runoff (responding to changes in climate variables at shorter timescales) but not total runoff (responding at longer time scales) (Touma et al., 2015) in defining compound hydrological drought and hot events. Thus, the assessment of changes based on soil moisture of different depths or total runoff (Berg and Sheffield, 2017; Wang and Miao, 2022; Zhao and Dai, 2022; Zhou et al., 2022) is also important to understand the future changes in CADHEs and CHDHEs. For example, for the future changes in CHDHEs based on total runoff (Fig. S7), we found that the change pattern is consistent with changes in CMDHEs in mid and high latitude regions, which is partly due to consistent changes between precipitation and total runoff in these regions (Cook et al., 2020; Wang et al., 2022), and differ from those based on surface runoff. Moreover, we select the period 1995–2014 as the reference period to assess the changes of future compound events in this study. Selecting different thresholds based on different reference periods may lead to a discrepancy in variations of extremes (Jones et al., 2012; Trenberth et al., 2014), including CDHEs (Feng et al., 2021). For example, a considerable positive bias can be found for CMDHEs in some regions (65.96 % of total grids) compared with GLDAS with relatively larger bias in Australia when applying the 1986–2005 as the reference period (commonly used in IPCC AR5 (IPCC, 2013)), as shown in Fig. S8.

5. Conclusion

Understanding how drought dynamics will change under persistent high temperatures in the future from a compound perspective is an important but rarely explored research area, which involves a series of complex processes (e.g., precipitation, soil moisture, and runoff) across disciplinary boundaries (climate, meteorology, and hydrology). Based on simulations from CMIP6 models and reference data from GLDAS, we evaluate the performance of models in simulating different types of compound droughts and hot events (CDHEs) and assess the future projection of the frequency and spatial extent of different types of CDHEs, including compound meteorological drought-hot events (CMDHEs), compound agricultural drought-hot events (CADHEs) and compound hydrological drought-hot events (CHDHEs), at the global scale under the SSP5-8.5 scenario. We found that CMIP6 climate models can reproduce the spatial distribution of three types of compound events compared with GLDAS. There is high consistency in the temporal changes of different CDHEs between CMIP6 and GLDAS, which indicates the relatively good performance of models in simulating temporal changes at the global scale (with a larger discrepancy in certain regions, such as

Australia). For the future projection under SSP5-8.5 scenarios, the frequency and spatial extent of three compound events show a marked increase during three future periods (with a relatively large increase in CADHEs and CHDHEs compared with CMDHEs). Globally, the average frequency of three compound events (i.e., CMDHEs, CADHEs, and CHDHEs) is projected to increase by 73.74 %, 113.95 %, and 114.17 % during the long term 2081–2100 relative to the base period 1995–2014 based on thirteen CMIP6 models, respectively. In addition, the uncertainty of CADHEs and CHDHEs is larger than CMDHEs in the future in most regions. Overall, the results of this study can provide useful insights into climate model performance for model developers. In addition, it also provides valuable information for stakeholders to anticipate the negative impacts of CDHEs and devise mitigation measures that alleviate the risks of compound extremes across different aspects of the hydrological cycle under global warming.

CRediT authorship contribution statement

Sifang Feng: Writing – original draft, Formal analysis. **Zengchao Hao:** Conceptualization, Formal analysis, Writing – original draft, Writing – review & editing. **Yitong Zhang:** Formal analysis. **Xuan Zhang:** Formal analysis. **Fanghua Hao:** Formal analysis.

Declaration of Competing Interest

The authors declare that they have no known competing financial interests or personal relationships that could have appeared to influence the work reported in this paper.

Data availability

I have shared the link to the data.

Acknowledgments

This research was funded by the National Natural Science Foundation of China (42271024). We thank the editor and reviewers for the constructive comments and suggestions. The Coupled Model Intercomparison Project (CMIP6) model simulations are obtained from https://esgf-node.llnl.gov/projects/cmip6/. The Global Land Data Assimilation System (GLDAS) dataset can be provided by (https://hydro1.gesdisc.eosdis.nasa.gov/data/GLDAS/GLDAS_NOAH025_M.2.0/).

Appendix A. Supplementary data

Supplementary data to this article can be found online at https://doi.org/10.1016/j.jhydrol.2023.129143.

References

Aadhar, S., Mishra, V., 2020. On the projected decline in droughts over South Asia in CMIP6 multimodel ensemble. J. Geophys. Res.-Atmos. 125 (20).
Afshar, M.H., Bulut, B., Duzenli, E., et al., 2022. Global spatiotemporal consistency between meteorological and soil moisture drought indices. Agric. For. Meteorol. 316, 108848.
Bastos, A., Ciais, P., Friedlingstein, P., et al., 2020. Direct and seasonal legacy effects of the 2018 heat wave and drought on European ecosystem productivity. Sci. Adv. 6 (24).
Berg, A., Sheffield, J., et al., 2017. Divergent surface and total soil moisture projections under global warming. Geophys. Res. Lett. 44 (1), 236–244.
Brunner, M.I., Swain, D.L., Gilleland, E., et al., 2021. Increasing importance of temperature as a contributor to the spatial extent of streamflow drought. Environ. Res. Lett. 16 (2), 024038.
Chen, S., Yuan, X., 2022. Quantifying the uncertainty of internal variability in future projections of seasonal soil moisture droughts over China. Sci. Total Environ. 824, 153817.
Cook, B.I., Mankin, J.S., Marvel, K., et al., 2020. Twenty-first century drought projections in the CMIP6 forcing scenarios. Earth's Future 8 (6).
Dai, A., 2013. Increasing drought under global warming in observations and models. Nat. Clim. Chang. 3 (1), 52–58.
Das, T., Pierce, D.W., Cayan, D.R., et al., 2011. The importance of warm season warming to western U.S. streamflow changes. Geophys. Res. Lett. 38 (23), L23403.
Dutta, R., Maity, R., 2022. Value addition in coupled model intercomparison project phase 6 over phase 5: global perspectives of precipitation, temperature and soil moisture fields. Acta Geophys. 70 (3), 1401–1415.
Feng, S., Hao, Z., Wu, X., et al., 2021. A multi-index evaluation of changes in compound dry and hot events of global maize areas. J. Hydrol. 602, 126728.
Feng, S., Hao, Z., Zhang, X., et al., 2022. Climate change impacts on concurrences of hydrological droughts and high temperature extremes in a semi-arid river basin of China. J. Arid Environ. 202, 104768.
Feng, S., Hao, Z., Meng, Y., et al., 2023. Increase in different hot droughts in the hydrological cycle largely explained by drought propagation. Water Resour. Res. Under review.
Fink, A.H., Brücher, T., Krüger, A., et al., 2004. The 2003 European summer heatwaves and drought –synoptic diagnosis and impacts. Weather 59 (8), 209–216.
Gevaert, A.I., Veldkamp, T.I.E., Ward, P.J., 2018. The effect of climate type on timescales of drought propagation in an ensemble of global hydrological models. Hydrol. Earth Syst. Sci. 22 (9), 4649–4665.
Greve, P., Kahil, T., Mochizuki, J., et al., 2018. Global assessment of water challenges under uncertainty in water scarcity projections. Nat. Sustain. 1 (9), 486–494.
Hao, Z., AghaKouchak, A., Phillips, T.J., 2013. Changes in concurrent monthly precipitation and temperature extremes. Environ. Res. Lett. 8 (3), 034014.
Hao, Z., Hao, F., Xia, Y., et al., 2022. Compound droughts and hot extremes: Characteristics, drivers, changes, and impacts. Earth Sci. Rev. 235, 104241.
Hou, Y., Guo, H., Yang, Y., et al., 2023. Global evaluation of runoff simulation from climate, hydrological and land surface models. Water Resour. Res. 59 (1).
Hua, L., Zhao, T., Zhong, L., 2022. Future changes in drought over Central Asia under CMIP6 forcing scenarios. J. Hydrol.: Reg. Stud. 43, 101191.
IPCC, 2013. Climate Change 2013: The Physical Science Basis. Contribution of Working Group I to the Fifth Assessment Report of the Intergovernmental Panel on Climate Change [Stocker T.F., D. Qin, G.-K. Plattner, M. Tignor, S.K. Allen, J. Boschung, A. Nauels, Y. Xia, V. Bex and P.M. Midgley (eds.)]. Cambridge University Press, Cambridge, UK and New York, NY, USA.
IPCC, 2021. Climate Change 2021: The Physical Science Basis. Contribution of Working Group I to the Sixth Assessment Report of the Intergovernmental Panel on Climate Change [Masson-Delmotte, V., P. Zhai, A. Pirani, S.L. Connors, C. Péan, S. Berger, N. Caud, Y. Chen, L. Goldfarb, M.I. Gomis, M. Huang, K. Leitzell, E. Lonnoy, J.B.R. Matthews, T.K. Maycock, T. Waterfield, O. Yelekçi, R. Yu, and B. Zhou (eds.)]. Cambridge University Press, Cambridge, UK and New York, NY, USA.
IPCC, 2022. Climate Change 2022: Impacts, Adaptation, and Vulnerability. Contribution of Working Group II to the Sixth Assessment Report of the Intergovernmental Panel on Climate Change [Pörtner H.-O. , D.C. Roberts, M. Tignor, E.S. Poloczanska, K. Mintenbeck, A. Alegría, M. Craig, S. Langsdorf, S. Löschke, V. Möller, A. Okem, B. Rama (eds.)], Cambridge University Press, Cambridge, UK and New York, NY, USA.
Iturbide, M., Gutiérrez, J.M., Alves, L.M., et al., 2020. An update of IPCC climate reference regions for subcontinental analysis of climate model data: definition and aggregated datasets. Earth Syst. Sci. Data 12 (4), 2959–2970.
Jones, P.D., Lister, D.H., Osborn, T.J., et al., 2012. Hemispheric and large-scale land-surface air temperature variations: An extensive revision and an update to 2010. J. Geophys. Res.-Atmos. 117 (D5), D05127.
Kendall, M.G., 1975. Rank correlation methods. Griffin, London.
Kirono, D.G.C., Hennessy, K.J., Grose, M.R., 2017. Increasing risk of months with low rainfall and high temperature in southeast Australia for the past 150 years. Clim. Risk Manage. 16, 10–21.
Koster, R.D., Suarez, M.J., Higgins, R.W., et al., 2003. Observational evidence that soil moisture variations affect precipitation. Geophys. Res. Lett. 30 (5), 1241.
Koster, R.D., Dirmeyer, P.A., Guo, Z., et al., 2004. Regions of strong coupling between soil moisture and precipitation. Science 305 (5687), 1138–1140.
Leonard, M., Westra, S., Phatak, A., et al., 2014. A compound event framework for understanding extreme impacts. Wiley Interdiscip. Rev.-Clim. Chang. 5 (1), 113–128.
Li, J., Bevacqua, E., Chen, C., et al., 2022. Regional asymmetry in the response of global vegetation growth to springtime compound climate events. Commun. Earth Environ. 3 (1), 123.
Li, X., Li, Z., 2022. Global water availability and its distribution under the Coupled Model Intercomparison Project Phase Six scenarios. Int. J. Climatol. 42 (11), 5748–5767.
Luo, L., Apps, D., Arcand, S., et al., 2017. Contribution of temperature and precipitation anomalies to the California drought during 2012–2015. Geophys. Res. Lett. 44 (7), 3184–3192.
Mann, H.B., 1945. Non-parametric tests against trend. Econometrica 13, 245–259.
Manning, C., Widmann, M., Bevacqua, E., et al., 2019. Increased probability of compound long-duration dry and hot events in Europe during summer (1950–2013). Environ. Res. Lett. 14 (9), 094006.
Mazdiyasni, O., AghaKouchak, A., 2015. Substantial increase in concurrent droughts and heatwaves in the United States. PNAS 112 (37), 11484–11489.
Meng, Y., Hao, Z., Feng, S., et al., 2022. Increase in compound dry-warm and wet-warm events under global warming in CMIP6 models. Glob. Planet. Change 210, 103773.
Miralles, D.G., Gentine, P., Seneviratne, S.I., et al., 2019. Land–atmospheric feedbacks during droughts and heatwaves: state of the science and current challenges. Ann. N. Y. Acad. Sci. 1436 (1), 19–35.
Mukherjee, S., Ashfaq, M., Mishra, A.K., 2020. Compound drought and heatwaves at a global scale: The role of natural climate variability-associated synoptic patterns and land-surface energy budget anomalies. J. Geophys. Res.-Atmos. 125 (11).
Mukherjee, S., Mishra, A.K., Ashfaq, M., et al., 2022. Relative effect of anthropogenic warming and natural climate variability to changes in compound drought and heatwaves. J. Hydrol. 605, 127396.

Muthuvel, D., Amai, M., 2022. Multivariate analysis of concurrent droughts and their effects on Kharif crops—A copula-based approach. Int. J. Climatol. 42 (5), 2773–2794.
Muthuvel, D., Sivakumar, B., Mahesha, A., 2023. Future global concurrent droughts and their effects on maize yield. Sci. Total Environ. 855, 158860.
Naumann, G., Alfieri, L., Wyser, K., et al., 2018. Global changes in drought conditions under different levels of warming. Geophys. Res. Lett. 45 (7), 3285–3296.
O'Neill, B.C., Tebaldi, C., van Vuuren, D.P., et al., 2016. The Scenario Model Intercomparison Project (ScenarioMIP) for CMIP6. Geosci. Model Dev. 9 (9), 3461–3482.
Poschlod, B., Zscheischler, J., Sillmann, J., et al., 2020. Climate change effects on hydrometeorological compound events over southern Norway. Weather Clim Extremes 100253.
Qiao, L., Zuo, Z., Xiao, D., 2022. Evaluation of soil moisture in CMIP6 simulations. J. Clim. 35 (2), 779–800.
Ridder, N.N., Pitman, A.J., Ukkola, A.M., 2021. Do CMIP6 climate models simulate global or regional compound events skillfully? Geophys. Res. Lett. 48 (2).
Ridder, N.N., Ukkola, A.M., Pitman, A.J., et al., 2022. Increased occurrence of high impact compound events under climate change. npj Clim. Atmos. Sci. 5 (1), 1–8.
Rodell, M., Houser, P.R., Jambor, U., et al., 2004. The global land data assimilation system. Bull. Amer. Meteorol. Soc. 85 (3), 381–394.
Sang, Y., Ren, H.-L., Shi, X., et al., 2021. Improvement of soil moisture simulation in Eurasia by the Beijing Climate Center Climate System Model from CMIP5 to CMIP6. Adv. Atmos. Sci. 38 (2), 237–252.
Sarhadi, A., Ausín, M.C., Wiper, M.P., et al., 2018. Multidimensional risk in a nonstationary climate: Joint probability of increasingly severe warm and dry conditions. Sci. Adv. 4 (11).
Shah, D., Mishra, V., 2020. Integrated Drought Index (IDI) for drought monitoring and assessment in India. Water Resour. Res. 56 (2).
Sippel, S., Reichstein, M., Ma, X., et al., 2018. Drought, heat, and the carbon cycle: a review. Curr. Clim. Chang. Rep. 4 (3), 266–286.
Spinoni, J., Naumann, G., Carrao, H., et al., 2014. World drought frequency, duration, and severity for 1951–2010. Int. J. Climatol. 34 (8), 2792–2804.
Stevenson, S., Coats, S., Touma, D., et al., 2022. Twenty-first century hydroclimate: A continually changing baseline, with more frequent extremes. Proc. Natl. Acad. Sci. 119 (12).
Touma, D., Ashfaq, M., Nayak, M.A., et al., 2015. A multi-model and multi-index evaluation of drought characteristics in the 21st century. J. Hydrol. 526, 196–207.
Trenberth, K.E., Dai, A., van der Schrier, G., et al., 2014. Global warming and changes in drought. Nat. Clim. Chang. 4 (1), 17–22.
Trenberth, K.E., Fasullo, J.T., 2012. Climate extremes and climate change: The Russian heat wave and other climate extremes of 2010. J. Geophys. Res.-Atmos. 117 (D17), D17103.
Ukkola, A.M., De Kauwe, M.G., Roderick, M.L., et al., 2020. Robust future changes in meteorological drought in CMIP6 projections despite uncertainty in precipitation. Geophys. Res. Lett. 47 (11).
Van Lanen, H.A.J., Wanders, N., Tallaksen, L.M., et al., 2013. Hydrological drought across the world: Impact of climate and physical catchment structure. Hydrol. Earth Syst. Sci. 17 (5), 1715–1732.
Van Loon, A.F., 2015. Hydrological drought explained. WIREs. Water 2 (4), 359–392.
Vicente-Serrano, S.M., Lopez-Moreno, J.-I., Beguería, S., et al., 2014. Evidence of increasing drought severity caused by temperature rise in southern Europe. Environ. Res. Lett. 9 (4), 044001.
Vicente-Serrano, S.M., Peña-Angulo, D., Beguería, S., et al., 2022. Global drought trends and future projections. Philos. Trans. A Math. Phys. Eng. Sci. 380 (2238), 20210285.
Vogel, M.M., Hauser, M., Seneviratne, S.I., 2020. Projected changes in hot, dry and wet extreme events' clusters in CMIP6 multi-model ensemble. Environ. Res. Lett. 15 (9), 094021.
Wang, A., Miao, Y., et al., 2022. Future changes in global runoff and runoff coefficient from CMIP6 multi-model simulation under SSP1-2.6 and SSP5-8.5 scenarios. Earth's. Future 10 (12).
Wang, T., Tu, X., Singh, V.P., et al., 2021. Global data assessment and analysis of drought characteristics based on CMIP6. J. Hydrol. 596, 126091.
Wang, L., Yuan, X., Xie, Z., et al., 2016. Increasing flash droughts over China during the recent global warming hiatus. Sci. Rep. 6 (1), 30571.
Weber, T., Bowyer, P., Rechid, D., et al., 2020. Analysis of compound climate extremes and exposed population in Africa under two different emission scenarios. Earth's Future 8 (9).
Woodhouse, C.A., Pederson, G.T., Morino, K., et al., 2016. Increasing influence of air temperature on upper Colorado River streamflow. Geophys. Res. Lett. 43 (5), 2174–2181.
Wu, J., Chen, X., Yao, H., et al., 2018. Hydrological drought instantaneous propagation speed based on the variable motion relationship of speed-time process. Water Resour. Res. 54 (11), 9549–9565.
Wu, Y., Miao, C., Sun, Y. et al., 2021c. Global observations and CMIP6 simulations of compound extremes of monthly temperature and precipitation. GeoHealth 5(5): e2021GH000390.
Wu, X., Hao, Z., Tang, Q., et al., 2021b. Projected increase in compound dry and hot events over global land areas. Int. J. Climatol. 41 (1), 393–403.
Wu, H., Su, X., Singh, V.P., 2021a. Blended dry and hot events index for monitoring dry-hot events over global land areas. Geophys. Res. Lett. 48 (24).
Yildirim, G., Rahman, A., Singh, V.P., 2022. Meteorological and hydrological drought hazard, frequency and propagation analysis: A case study in southeast Australia. J. Hydrol.: Reg. Stud. 44, 101229.
Yuan, S., Quiring, S.M., Leasor, Z.T., 2021. Historical changes in surface soil moisture over the contiguous United States: An assessment of CMIP6. Geophys. Res. Lett. 48 (1).
Yuan, X., Wang, L., Wood, E.F., 2018. Anthropogenic intensification of Southern African flash droughts as exemplified by the 2015/16 season. Bull. Amer. Meteorol. Soc. 99 (1), S86–S90.
Zeng, J., Li, J., Lu, X., et al., 2022. Assessment of global meteorological, hydrological and agricultural drought under future warming based on CMIP6. Atmos. Ocean. Sci. Lett. 15 (1), 100143.
Zhan, W., He, X., Sheffield, J., et al., 2020. Projected seasonal changes in large-scale global precipitation and temperature extremes based on the CMIP5 ensemble. J. Clim. 33 (13), 5651–5671.
Zhang, J., Wang, W.-C., Wei, J., 2008. Assessing land-atmosphere coupling using soil moisture from the Global Land Data Assimilation System and observational precipitation. J. Geophys. Res.-Atmos. 113 (D17), D17119.
Zhang, J., Chen, H., Zhang, Q., 2019. Extreme drought in the recent two decades in northern China resulting from Eurasian warming. Clim. Dyn. 52 (5), 2885–2902.
Zhang, Q., She, D., Zhang, L., et al., 2022. High sensitivity of compound drought and heatwave events to global warming in the future. Earth's Future 10 (11).
Zhao, T., Dai, A., 2022. CMIP6 Model-projected hydroclimatic and drought changes and their causes in the twenty-first century. J. Clim. 35 (3), 897–921.
Zhou, S., Zhang, Y., Park Williams, A., et al., 2019. Projected increases in intensity, frequency, and terrestrial carbon costs of compound drought and aridity events. Sci. Adv. 5 (1).
Zhou, S., Williams, A.P., Lintner, B.R., et al., 2022. Diminishing seasonality of subtropical water availability in a warmer world dominated by soil moisture–atmosphere feedbacks. Nat. Commun. 13 (1), 1–10.
Zhu, Y., Liu, Y., Wang, W., et al., 2021. A global perspective on the probability of propagation of drought: From meteorological to soil moisture. J. Hydrol. 603.
Zscheischler, J., Martius, O., Westra, S., et al., 2020. A typology of compound weather and climate events. Nat. Rev. Earth. Environ. 1 (7), 333–347.
Zscheischler, J., Seneviratne, S.I., 2017. Dependence of drivers affects risks associated with compound events. Sci. Adv. 3 (6).
Zscheischler, J., Westra, S., van den Hurk, B.J.J.M., et al., 2018. Future climate risk from compound events. Nat. Clim. Chang. 8 (6), 469–477.